IAI Journals.ASM.org

Mycobacterial Trehalose Dimycolate Reprograms Macrophage Global Gene Expression and Activates Matrix Metalloproteinases

Kaori Sakamoto,[a] Mi Jeong Kim,[b] Elizabeth R. Rhoades,[c] Rachel E. Allavena,[d] Sabine Ehrt,[e] Helen C. Wainwright,[e] David G. Russell,[f] Kyle H. Rohde[g]

Department of Pathology, College of Veterinary Medicine, University of Georgia, Athens, Georgia, USA[a]; Department of Immunobiology, Joslin Diabetes Center, Harvard Medical School, Boston, Massachusetts, USA[b]; Cornell NanoScale Science and Technology Facility, Cornell University, Ithaca, New York, USA[c]; School of Veterinary Science, University of Queensland, Gatton, Queensland, Australia[d]; Department of Microbiology and Immunology, Weill Cornell Medical College, New York, New York, USA[e]; Groote Schuur Hospital, University of Cape Town, Cape Town, South Africa[e]; Department of Microbiology and Immunology, Veterinary Medical Center, Cornell University, Ithaca, New York[f]; Burnett School of Biomedical Sciences, College of Medicine, University of Central Florida, Orlando, Florida, USA[g]

Trehalose 6,6′-dimycolate (TDM) is a cell wall glycolipid and an important virulence factor of mycobacteria. In order to study the role of TDM in the innate immune response to *Mycobacterium tuberculosis*, microarray analysis was used to examine gene regulation in murine bone marrow-derived macrophages in response to 90-μm-diameter polystyrene microspheres coated with TDM. A large number of genes, particularly those involved in the immune response and macrophage function, were up- or downregulated in response to these TDM-coated beads compared to control beads. Genes involved in the immune response were specifically upregulated in a myeloid differentiation primary response gene 88 (MyD88)-dependent manner. The complexity of the transcriptional response also increased greatly between 2 and 24 h. Matrix metalloproteinases (MMPs) were significantly upregulated at both time points, and this was confirmed by quantitative real-time reverse transcription-PCR (RT-PCR). Using an *in vivo* Matrigel granuloma model, the presence and activity of MMP-9 were examined by immunohistochemistry and *in situ* zymography (ISZ), respectively. We found that TDM-coated beads induced MMP-9 expression and activity in Matrigel granulomas. Macrophages were primarily responsible for MMP-9 expression, as granulomas from neutrophil-depleted mice showed staining patterns similar to that for wild-type mice. The relevance of these observations to human disease is supported by the similar induction of MMP-9 in human caseous tuberculosis (TB) granulomas. Given that MMPs likely play an important role in both the construction and breakdown of tuberculous granulomas, our results suggest that TDM may drive MMP expression during TB pathogenesis.

Mycobacterium tuberculosis, the causative agent of tuberculosis (TB), infects approximately one-third of the human population and is the leading bacterial cause of human mortality worldwide, killing 1.45 million individuals per year (1). In the majority of cases, however, the bacteria are sequestered within a well-organized granuloma, where they can remain in a poorly characterized, "latent" state for decades. The granuloma structure is typically composed of centrally located, infected macrophages in various stages of degeneration and necrosis, surrounded by epithelioid macrophages, foamy macrophages, and occasional multinucleated giant cells, all bordered by a mixed population of lymphocytes and a fibrous capsule. This capsule consists of a wall of collagen that is laid down by fibroblasts and must be broken down in order for transmission to occur. Infected individuals who are immunocompetent and/or treated can resolve granulomas, with disaggregation of the accumulated leukocytes, dissolution of the extracellular matrix, and either scar formation or a return to the normal pulmonary architecture. In progressively infected individuals, on the other hand, the granuloma liquefies, the capsule wall cavitates and ruptures into an adjacent airway, and the bacilli multiply and are released (2). While some causes of tuberculosis reactivation are known, such as coinfection with human immunodeficiency virus (3), aging, chemotherapy, malignant disease, malnutrition, and other causes of immunosuppression, in many cases the "trigger" leading to the breakdown of the granuloma capsule is unknown.

Trehalose 6,6′-dimycolate (TDM) is a major glycolipid present in the cell walls of mycobacteria and other members of the order *Actinomycetales*. TDM confers a cording (clumped) phenotype to virulent mycobacterial species and has been shown to produce many of the clinical signs and lesions associated with TB and complete Freund's adjuvant (4, 5). Intriguingly, the proinflammatory activity of TDM is dependent upon its mode of presentation to immune cells; larger surface areas of presentation, such as monolayers, emulsions, and nonphagocytosable particles, are more stimulatory than micelles or bacterium-sized particles (6–8). Histopathologic and microarray analyses of artificial granulomas, induced in mice by the injection of TDM-coated beads admixed with Matrigel, showed that TDM elicits foam cell formation and regulation of some of the host lipid metabolism genes in a manner similar to that observed in human TB granulomas (9). The exact role of TDM in the pathogenesis of TB, however, remains to be determined.

Matrix metalloproteinases (MMPs) are a family of zinc metalloendopeptidases secreted by a variety of cells that function in the turnover of extracellular matrix components, making MMPs

Received 29 August 2012 **Returned for modification** 26 September 2012
Accepted 18 December 2012
Published ahead of print 21 December 2012
Editor: B. A. McCormick
Address correspondence to Kaori Sakamoto, kaoris@uga.edu.

doi:10.1128/IAI.00906-12

likely players in cavity formation and the breakdown of the granuloma capsule. MMPs are also involved in cell migration, intercellular communication, and a variety of pathological conditions (10). The MMPs are classified into subgroups based on their structure and substrate specificities (collagenases, gelatinases, stromelysins, matrilysins, membrane-type MMPs, etc.). Most MMPs are not expressed in normal healthy tissues but are expressed and activated in tissues that are inflamed or undergoing remodeling. MMPs can be upregulated by various exogenous stimuli, such as bacterial components, cytokines, or cell-to-cell contact. MMP secretion is regulated primarily by the prostaglandin and mitogen-activated protein kinase (MAPK) signal transduction pathways (11).

As MMPs can be highly destructive, the process of activation is tightly regulated. First, with the exception of MMP-8 and -9, the MMPs are not stored and require *de novo* gene transcription. Second, MMPs are synthesized as zymogens and must have their N-terminal propeptide removed by other MMPs or proteinases in order to become active (12). Finally, there are endogenous inhibitors of MMP activity, such as α2-macroglobulin, as well as the four specific tissue inhibitors of metalloproteinases (TIMPs) identified in humans to date (13), which inhibit MMP activity by binding to the catalytic site (14). MMPs may also be inactivated by internalization or oxidation and downregulated by certain cytokines, such as gamma interferon (IFN-γ), interleukin-4 (IL-4), and IL-10 (15, 16).

The pulmonary parenchyma is rich in collagen types I, III, and IV, as well as elastin. It is therefore likely that MMPs that can cleave these fibrils are involved in tuberculosis granuloma formation, cavitation, and capsule breakdown. In mice, *M. tuberculosis* infection results in increased MMP-2 and -9 (gelatinases) levels (17, 18). In human TB studies, MMP-1 (interstitial collagenase not present in mice), MMP-2, MMP-7 (matrilysin), MMP-8 (neutrophil elastase), and MMP-9 have been described as being upregulated either *in vitro* or *in vivo* (19–22). Recently, the importance of MMP-1 was highlighted in a report showing that *M. tuberculosis* infection of MMP-1 transgenic mice caused more destructive lesions with greater similarity to TB lesions in humans (23) than those observed in wild-type mice. Circulating levels of MMP-9, in particular, have been shown to correlate with disease severity in tuberculosis patients (24). MMP-9 has also been shown in the zebrafish model to be induced by the mycobacterial virulence factor 6-kDa early secreted antigenic target (ESAT6), which plays a significant role in macrophage recruitment, granuloma formation, and bacterial survival (25).

In this study, we used DNA microarrays to compare murine bone marrow-derived macrophage (BMMΦ) transcriptional responses to TDM-coated microspheres with those to phosphatidylglycerol (PG)-coated microspheres or those of resting macrophages at early (2 h) and late (24 h) time points. The transcriptional responses to TDM in mice deficient in the Toll-like receptor (TLR) adaptor molecule myeloid differentiation primary response gene 88 (MyD88) versus wild-type BMMΦ responses were also compared. These experiments revealed that many immune response and tissue remodeling genes were upregulated in a MyD88-dependent manner after stimulation with TDM. The marked upregulation of MMP-8, -9, -12, -13, and -14 in response to TDM, which was validated by real-time reverse transcription-PCR (RT-PCR), prompted further study of these related enzymes. A murine Matrigel-based granuloma model was used to show that TDM induces production of MMP-8 and -9, and activation of MMP-9 was specifically shown by *in situ* zymography (ISZ). Moreover, MMP-9 was also determined, by laser capture microdissection and microarray analysis, to be highly upregulated in late-stage human TB granulomas. Based on these results, we propose that in late-stage TB granulomas, large aggregates of *M. tuberculosis* or mycobacterial lipids within the caseous core could provide a large surface area of TDM presentation to macrophages, stimulating them to produce and activate various MMPs, which may in turn break down the capsule, leading to TB transmission.

MATERIALS AND METHODS

Mice. C57BL/6 mice were purchased from Charles River Breeding Laboratories or Taconic. MyD88-deficient mice on a C57BL/6/129F2 background were generated by S. Akira (Osaka University) and generously provided by S. Ehrt (Weill Cornell Medical College). All mice were housed at the Cornell University Transgenic Mouse Facility under specific-pathogen-free conditions. All mice used in this study were between 5 and 8 weeks of age.

Human TB granulomas. Data from human tissue specimens were mined from a previously published microarray study (9). That work was approved by the institutional review boards at the University of Cape Town, South Africa, the Public Health Research Institute, Newark, NJ, and Cornell University, Ithaca, NY. Informed consent was obtained from all patients.

Macrophage culture. BMMΦ were cultured as previously described (8) and maintained in Dulbecco's modified Eagle's medium supplemented with L-929 cell-conditioned medium (20%), 10% heat-inactivated fetal calf serum (FCS; HyClone), L-glutamine (2 mM; Gibco), sodium pyruvate (1 mM; Gibco), 100 U/ml penicillin (Gibco), and 100 μg/ml streptomycin (Gibco).

Lipid extraction and purification. *Mycobacterium bovis* BCG Pasteur or *M. tuberculosis* H37Rv cultures were grown in shaking liquid cultures of Middlebrook 7H9 (Difco) or glycerol-alanine-salts (GAS) medium, respectively, as previously described (8, 26). The bacilli were washed extensively with phosphate-buffered saline (PBS) before extraction with chloroform and methanol, fractionation, and purification as previously described (8, 27). Purified lipid identities were confirmed by Fong Hsu at Washington University, using electrospray ionization mass spectrometry. Bovine-derived PG and *M. tuberculosis* H37Rv TDM (for some experiments) were purchased from Sigma-Aldrich. All lipids were stored in chloroform-methanol (2:1 [vol/vol]) at 10 mg/ml at −20°C under nitrogen.

Lipid-coated microspheres. A total of 125 μg of either *M. bovis* BCG TDM, *M. tuberculosis* H37Rv TDM, or PG solubilized in chloroform-methanol (2:1 [vol/vol]) was used to coat the surfaces of solvent-resistant tubes. A total of 2.5 ml of a 2.5% solids solution of 90-μm-diameter polystyrene microspheres (Polysciences) for each sample was washed twice with PBS and then coated with the lipids as previously described (8). Lipid-coated microspheres were resuspended in 1 ml of PBS.

BMMΦ RNA extraction. Lipid-coated microspheres were added to 60-mm-diameter dishes (non-tissue culture treated; Kord-Valmark) of confluent BMMΦ that had been acclimated for at least 1 h to 4 ml of fresh warmed medium. For 2-h experiments, the medium was discarded and immediately replaced with 4 ml of TRIzol (Invitrogen), with pipetting and rinsing to lyse the cells completely. Lysates were immediately transferred to solvent-resistant tubes and frozen at −80°C until RNA extraction. For 24-h experiments, the medium was brought up to 10 ml 2 h after adding the microspheres, and then the cells were lysed after 24 h as described above. RNA was extracted using an RNeasy minikit (Qiagen) and then treated with Turbo DNA-free DNase (Ambion) following the manufacturers' instructions.

Microarray analysis. All RNA samples were submitted to the Cornell University Core Microarray Facility for processing and microarray analysis. RNA purity and integrity were examined on an Agilent Bioanalyzer 2100. Total RNA samples were labeled using a MessageAmp II-Biotin Enhanced Single Round aRNA amplification kit (Ambion, Austin, TX) according to the manufacturer's protocol. Labeled cRNA was hybridized

on Affymetrix mouse MG430A 2.0 (or other) GeneChips, stained, washed, and scanned by a GeneChip Scanner 3000. The raw array data were processed by Affymetrix GCOS software to obtain detection calls and signal values. The signals of each array were normalized by scaling to a target value of 500, using GCOS software. Files were preprocessed with the GC-RMA algorithm and analyzed with Genespring 7.3 (Agilent Technologies) software. Data from human TB granulomas were analyzed as previously described (9). Each microarray data set represents the averages for three independent biological replicates with separate RNA isolation, labeling, and array hybridization. Genes with significant changes in gene expression were identified based on a combination of fold change and *P* value cutoffs and analysis of variance (ANOVA), as indicated in the text.

Real-time RT-PCR. cDNA was synthesized from 250 ng total RNA by use of an iScript cDNA synthesis kit (Bio-Rad), using the following temperature cycle: 25°C for 5 min, 42°C for 30 min, and 85°C for 5 min. iTaq SYBR Green Super mix with ROX (Bio-Rad) was used per the manufacturer's protocol, with 2 μl sample cDNA and a 7.2 μM final concentration of primer. Relative quantitative real-time PCR was performed using an ABI 7500 thermal cycler (Applied Biosystems) following the manufacturer's protocol, with β-actin as an endogenous control. Dissociation curves were run after each assay per the manufacturer's instructions for quality control. Primer sequences are available upon request. All primers used were optimized by comparing amplification efficiencies between endogenous controls and target RNA over a dose range. Results present the averages for three technical replicates and are representative of three biological replicates.

Bead-based granuloma model. One hundred micrograms of *M. tuberculosis* H37Rv TDM (Sigma-Aldrich) was used to coat solvent-resistant tubes, to which were added 2×10^3 90-μm-diameter or 3×10^6 10-μm-diameter washed polystyrene microspheres suspended in 1 ml of PBS. For immunohistochemistry (IHC)-based experiments, 10^7 congenic BMMΦ were added to this Matrigel solution, and injections were performed intraperitoneally (i.p.). Ninety-micrometer-diameter microspheres were required for i.p. injections, as microspheres with smaller diameters do not allow cohesiveness of the matrix in the peritoneal cavity. The i.p. granuloma model is also consistent with and comparable to our previous work (7, 8). For ISZ experiments, cryosectioning was required, which could not be performed with 90-μm-diameter microspheres; 10-μm-diameter spheres, which have previously been shown to be immunostimulatory (8), although less so than 90-μm-diameter microspheres, were used instead, and injections were given subcutaneously to avoid dispersal of the matrix. Histologically, subcutaneous matrices are comparable to peritoneal ones, as similar leukocyte populations are recruited to 10-μm-diameter spheres, in a comparable time frame. Microspheres were coated as described previously (8), with the exception of extra sonication steps to resuspend the 10-μm-diameter coated beads after each centrifugation. TDM-coated microspheres were then resuspended in 1 ml of growth factor-reduced Matrigel (BD Biosciences), drawn up in 1-ml TB syringes fitted with 21-gauge needles, and kept on ice until injection. Three hundred microliters of this matrix was injected per mouse. For ISZ, no BMMΦ were added so that only recruited leukocytes were examined for MMP activity. At various time points, injected mice were euthanized and the artificial granulomas were either placed in 4% paraformaldehyde (PFA) in PBS for IHC or snap-frozen in Tissue-Tek OCT compound (Sakura) in liquid nitrogen for ISZ. For IHC, samples were kept in 4% PFA at 4°C for at least 24 h, transferred to 70% ethanol for at least 24 h, and then submitted to the Histology Laboratory at the Cornell University Diagnostic Laboratory for processing. ISZ samples were maintained at −80°C until cryosectioning.

Neutrophil depletion. An anti-Ly-6G antibody (rat IgG2b, clone RB6-8C5) was developed by R. Coffman (DNAX Research Institute). This antibody (RB6) depletes murine neutrophils and eosinophils as well as a subset of macrophages *in vivo* (28, 29). RB6-8C5 hybridoma cells, generously provided by E. Denkers (Cornell University), were cultured in hybridoma SFM (Gibco Life Technologies) in Vectracell single-use bioreactors (Vectracell). Hybridoma supernatants were filtered through 0.2-μm-pore-size filters prior to storage at 4°C until RB6 antibody recovery. Antibody was concentrated using an Amicon 8400 device (Millipore) fitted with a 100-kDa exclusion membrane (Millipore-Amicon YM100 ultrafiltration membrane). Antibody purity was confirmed by SDS-PAGE before further concentration using an Amicon Ultra-15 centrifugal filter device with a nominal molecular weight limit (NMWL) of 30,000 (Millipore). Antibody concentration was determined by Bradford assay (Bio-Rad), and the antibody was resuspended at 2 mg/ml in PBS, sterile filtered, and stored at 4°C until use. C57BL/6 mice were injected i.p. with 200 μg of RB6 suspended in 100 μl of PBS at intervals of 48 h until sacrifice. These mice were injected with TDM-coated bead matrices (as described above) 48 h after the first RB6 dose. Mice were sacrificed at 14 h, 36 h, and 4 days post-matrix injection. Depletion of neutrophils and subsets of eosinophils and macrophages was confirmed by flow cytometry. Matrices were fixed and processed for IHC as described above.

ISZ. Cryosections were thawed and air dried. OCT was dissolved by incubating slides in PBS for 1 h at room temperature. Sections were preincubated with ISZ buffer (ISZB; 50 mM Tris, pH 7.4, 10 mM $CaCl_2$, 0.05% Triton X-100) with or without inhibitors for 1 h at room temperature. For MMP-9, frozen aliquots of DQ-gelatin buffer (2% gelatin, 2% sucrose, 0.02% sodium azide in PBS) and DQ-gelatin (0.025% DQ-gelatin in buffer) were thawed at 100°C and then transferred to and maintained at 50°C until used. For other MMPs, aliquots of 1% agarose in ISZB were thawed as described above. Inhibitors and exogenous MMPs (positive controls) were also thawed at 50°C and used at final concentrations of 60 nM (MMP-2/9 inhibitor), 40 nM (MMP-8 inhibitor), and 0.4 mg/ml (exogenous MMPs). Slides were dried by blotting around the section and were warmed on a 37°C heat block. Twenty-five microliters of DQ-gelatin or agarose mix, with or without inhibitors or exogenous MMPs, was applied to each section on the 37°C heat block and immediately coverslipped and sealed with nail polish. Slides were maintained in the dark in a humidity chamber at 37°C for 1 h (MMP-9) or 24 h (others) before being examined by fluorescence microscopy on a Zeiss Axioskop 2 Plus microscope. Images for ISZ and IHC were taken using an AxioCam camera and Axiovision software (Zeiss). All images were obtained using the same exposure time.

Immunohistochemistry. Paraffin-embedded sections were deparaffinized in xylene and rehydrated sequentially in 100%, 95%, and 70% ethanol and then water. Endogenous peroxide was blocked by immersion of the sections in 0.5% hydrogen peroxide in methanol for 10 min. Antigen retrieval methods involved incubation with trypsin (Zymed kit) for 20 min at 37°C, followed by three 5-min washes in 0.05% Tween-PBS. Sections were blocked using 10% normal goat serum with 2× casein for 20 min at room temperature. Primary rabbit anti-mouse MMP-8 or -9 antibodies or isotype control antibodies were diluted 1:50 or 1:100 in PBS with 1× casein and applied to sections for 1.5 to 2 h at 37°C. A biotinylated goat anti-rabbit secondary antibody (Vector Laboratories) was used at 1:200 in PBS for 20 min at room temperature, followed by streptavidin peroxidase (Zymed) for 20 min at room temperature. Sections were developed using AEC chromogen/substrate solution (Zymed) at room temperature for 5 to 15 min. The reaction was stopped using distilled water, and then the sections were counterstained using Gill's number 2 hematoxylin (Fisher) for 30 s, rinsed under water, and mounted using Fluoromount (Fisher).

Microarray data accession numbers. The raw data from these DNA microarray experiments have been deposited in the ArrayExpress database (http://www.ebi.ac.uk/arrayexpress/) under accession numbers E-MEXP-3815 for the MyD88 experiments and E-MEXP-3814 for all other experiments.

RESULTS

Trehalose dimycolate induces the regulation of a unique set of macrophage genes. While immunostimulatory effects of TDM are well studied, a comprehensive examination of macrophage gene regulation by TDM has not been performed. In an effort to

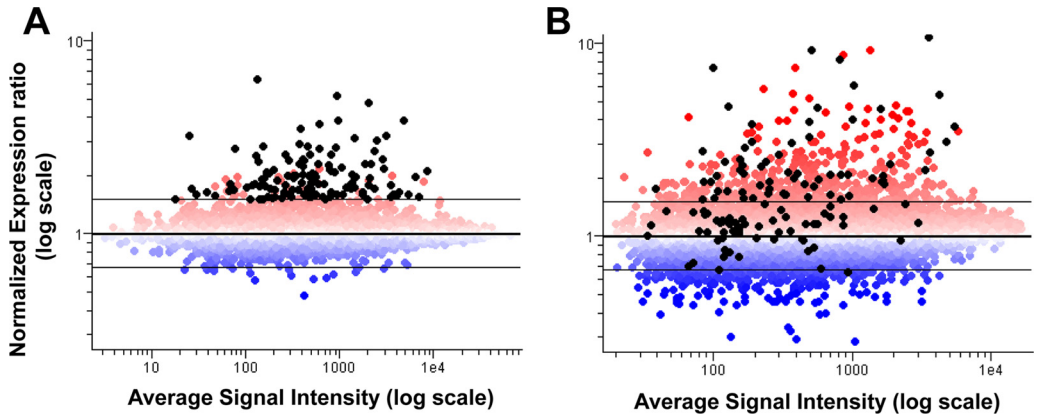

FIG 1 Macrophage gene regulation in response to TDM. BMMΦ from C57BL/6 mice were stimulated with 90-μm-diameter microspheres coated with TDM purified from *M. tuberculosis* strain H37Rv for either 2 (A) or 24 (B) hours. Dots represent individual genes, with red indicating upregulated genes and blue indicating downregulated genes, after normalization for gene regulation in response to PG-coated microspheres. The horizontal lines above and below 1 on the *y* axis indicate our 1.5-fold cutoffs. Black dots indicate genes upregulated at 2 h that meet the criterion of a *P* value of <0.05.

understand how TDM stimulates macrophages, we examined the regulation of genes in murine BMMΦ in response to *M. tuberculosis* H37Rv TDM-coated, 90-μm-diameter microspheres at early (2 h) and late (24 h) time points. We compared these data with the response to microspheres coated with phosphatidylglycerol (PG), a relatively noninflammatory lipid, as a control for nonspecific gene regulation induced by the phagocytosis of a lipid and exposure to polystyrene microspheres. PG elicits minimal leukocyte recruitment or cytokine production in this microsphere model (7, 8).

Our data indicated that 125 murine genes were upregulated over 1.5-fold ($P < 0.05$) in response to TDM, as early as 2 h after exposure (Fig. 1A). By 24 h, a substantial number of genes were either upregulated (503 genes were upregulated >1.5-fold; $P < 0.05$) or downregulated (162 genes were downregulated >1.5-fold; $P < 0.05$) in response to H37Rv TDM (Fig. 1B). Table 1 lists the specific genes, organized by biological process, that were upregulated at least 1.5-fold ($P < 0.05$) at 2 h by TDM-coated beads compared to PG-coated bead controls. Most of these genes are involved in the acute inflammatory response. Very few genes were downregulated by TDM-coated beads at 2 h, and these included genes encoding the transcriptional regulators Mafb (v-maf musculoaponeurotic fibrosarcoma oncogene family, protein B) and Id1 (inhibitor of DNA binding 1), the endopeptidase Enc1 (ectodermal-neural cortex 1), an immediate-early response 5-like gene product, dual specificity phosphatase 6, SH3 domain binding protein 5, and thrombomodulin.

Genes upregulated at 24 h and with relevance to the immune response are listed in Table 2, and relative up- or downregulation of genes involved in the immune response and macrophage function between 2 and 24 h is shown in Fig. 2. Specific genes with relevance to host responses to *M. tuberculosis* and that were up- or downregulated at both 2 and 24 h are shown in Fig. 3. Intriguingly, the macrophage receptor with collagenous structure (MARCO), a class A scavenger receptor that we recently showed to bind and aid in the macrophage response to TDM (30), was markedly upregulated between 2 and 24 h (Fig. 3E).

Approximately 30 genes were downregulated at least 2-fold in response to TDM-coated beads at 24 h, and genes of interest with regard to immune responses and tissue remodeling are listed in Table 3. Interestingly, the gene for thrombomodulin, which is a component of the anticoagulation pathway, was the only downregulated gene from 2 h that continued to be downregulated at 24 h. This was not surprising, as tumor necrosis factor alpha (TNF-α), which is one of the major cytokines induced in response to TDM (8), can inhibit thrombomodulin expression in order to enhance coagulation during inflammatory responses (31).

While many of the genes overlapped between the two time points, we noted distinct temporal patterns of gene expression in response to treatment with TDM-coated beads (Fig. 2). ANOVA comparing data from 2 h versus 24 h revealed about 450 genes with significantly different expression levels over time (>1.5-fold; $P < 0.05$) (Fig. 2A). This was seen in the diverse behaviors of early-induced genes after prolonged stimulation by TDM-coated beads. In Fig. 1B, it is notable that while some genes induced at 2 h (shown as black dots) remained elevated at 24 h, others returned to control levels. By 24 h posttreatment, a subset of genes induced at 2 h was repressed below control levels (Fig. 2B, cluster 1). There were 51 genes exhibiting sustained upregulation (>1.5-fold; $P < 0.05$) at both 2 and 24 h (Fig. 2B, clusters 2 and 3, and C, cluster 3). Of these, 27 genes with sustained induction were even more highly expressed at 24 h (Fig. 2B, cluster 3, and Table 1, asterisks), including genes that have been shown to play a role during TB or are induced by *M. tuberculosis* infection or stimulation with mycobacterial components, such as the genes encoding TNF-α (32), CXCL10 (IP-10) (33), Nfkbia (34), Rel-b (35), ICAM-1 (36), and prostaglandin-endoperoxide synthase 2 (ptgs2) (37). The predominant profile encompassed a large number of genes displaying delayed induction 24 h after exposure to TDM (Fig. 2C, clusters 1 and 2).

Transcriptional responses to TDM are predominantly MyD88 dependent. The highly proinflammatory nature of TDM and our previous data showing MyD88-dependent proinflammatory cytokine induction by TDM-coated beads (8) prompted us to examine differences in gene regulation between MyD88$^{-/-}$ and wild-type BMMΦ in response to TDM-coated microspheres at 24 h. Negative controls in this independent set of experiments were resting macrophages of the same genotype. Because this design did not account for changes triggered by bead phagocytosis unrelated to TDM, however, only genes shown in the experiment described

TABLE 1 BMMΦ genes upregulated in response to 90-μm-diameter, H37Rv TDM-coated beads at 2 h[a]

Functional category and gene product	Fold change
Immune response	
Cytokines	
IL-1beta	5.21
IL-1rn	1.56
IL-10	1.8
MCSF-1*	1.94
TNF*	3.02
Chemokines	
CCL3	2.42
CCL4	2.69
CCL7	1.82
CCL12	2.12
CCRl2*	2.01
CXCL1	4.75
CXCL2†*	3.84
CXCL10*	2.8
Others	
BC008167	1.63
CD40	1.6
Clec4e*	2.27
Irf1†	1.89
Mefv*	1.8
SOD2*	1.56
Tnfsf9	2.74
Signaling	
Acvr2a	1.64
Adora2b	2.29
Cav1*	1.81
Cdc42ep4	1.82
Cish	2.1
Dscr1	1.56
Dusp1	1.59
Dusp16	1.52
Dusp2	1.98
Erbb2ip	1.64
Gpr84*	3.11
Pde4b*	3.47
Pim1	2.15
Rab20*	2.07
Ralgds	1.68
Rgs16	1.63
Rgs3	1.51
Rrad	1.72
Snag1	1.55
Socs3	4.03
Spata13*	1.99
Protein modification	
Herpud1	1.55
Transcription	
Bcl3†	1.96
Btg2	1.6
Egr1	1.84
Egr2	1.75
Jun dimerization protein 2†	1.7
Klf7	1.94
Maff†	2.82
Nfkbia*	1.96
Nfkbie*	2.57
Nfkbiz	2.67
Prdm1	2.44
Rel	2.05
Relb*	2.01
Rpl35	1.7
Zc3h12a	1.63
Cell proliferation	
Ets2	1.58
Gadd45b	1.91
Junb	1.83
Pdgfb	2.08
Trim13†*	2.05
Cell interactions	
Icam1*	2.17
Pvr	1.69
Proteolysis	
BB637972	3.23
Carboxypeptidase D	1.65
MMP13	1.72
MMP14*	2.76
Serpinb6b	1.55
Timp1	1.74
Tnfaip3	2.51
Apoptosis	
Birc3	1.93
Cflar*	2.16
Cias1	2.02
Hspa1b*	2.43
Phlda1	2.1
Plagl2	1.84
Ripk2	1.54
Traf1	2.41
DNA repair	
Hspa1a	2.34
Sfpq	1.78
Lipid metabolism	
Ch25h	2.91
Ptgs2*	6.28
Saa3*	1.92
Angiogenesis	
Qk	1.67
Tnfaip2*	1.56
Unknown	
AA200306	1.57
BB183628	2.83
BC025514	1.83
BE196832	1.83
BE631223	1.8
Brd4	1.68
CD83	1.63
Errfi1	1.86
Ibrdc3*	1.73
Ier3	2.3
Irg1†*	3.19
Luc7l2	1.62
Marcksl1*	1.64
NM_138648	4.83
Nupr1	2.4
Tnip1	1.6

[a] Data for all upregulated genes are shown. Data for replicate genes were averaged. Genes are listed by gene product and categorized according to predominant biological functions with relevance to this study. Genes in common with the response to LPS at 2 h (†) and genes that continue to increase at 24 h (*) are marked.

above to be specifically up- or downregulated in response to TDM were further analyzed. As shown in Fig. 4A, there were tremendous alterations in gene expression in response to TDM-coated beads in wild-type BMMΦ controls. In contrast, in the absence of

TABLE 2 BMMΦ immune response genes upregulated at least 2-fold by H37Rv TDM-coated beads compared to PG-coated beads at 24 h[a]

Immune response gene product	Fold change
C3	4.77
CCRl2	3.64
Clec4e	7.11
Clec4n	4.44
Csf1	2.43
Csf2rb1	2.02
Csf2rb2	2.35
Cxcl10	6.07
Cxcl2	4.57
Gca	2.41
Icam1	2.08
Ifi35	2.38
Ifi47	2.74
Ifih1	2.47
Ifit1	4.83
Ifit2	3.58
Ifit3	5.08
IL18bp	2.25
Irf7	4.11
Irgm	2.67
Mefv	2.75
Oas1a	2.1
Oas3	3.41
Pla2g7	3.2
Relb	2.08
Sod2	3.09
Stat1	3.1
Stat2	2.98
TLR2	2.21
TNF	3.03

[a] Genes were categorized according to the GO biological process listings in GeneSpring (Agilent).

MyD88, we observed a dramatically muted transcriptional response to TDM (Fig. 4B). Most of the genes involved in immune and inflammatory responses, in particular (Fig. 4, black dots), required MyD88. Furthermore, most of the genes both up- and downregulated in response to TDM at 24 h were also MyD88 dependent (Fig. 5). These results support our previous work showing that TDM interacts with and signals through MARCO, TLR2, and CD14, in a MyD88-dependent manner (30), which has been refuted by proponents of Mincle as the TDM receptor on macrophages (38, 39). Interestingly, key chemokines involved in the TB response, such as CXCL1 and CCL5, were not MyD88 dependent, suggesting that TDM stimulates additional MyD88-independent immune signaling pathways.

TDM induces marked upregulation of MMPs in macrophages. Upon inspection of the list of genes upregulated in wild-type BMMΦ in response to TDM-coated beads relative to resting BMMΦ, it was observed that several MMPs (MMPs 8, 9, 12, 13, 14, and 19) were markedly upregulated at 24 h, in a MyD88-dependent manner (Fig. 6). These genes were also upregulated in response to TDM in an experiment using cells that had been exposed to PG-coated beads as a control for genes upregulated in response to phagocytosis of a lipid, and they were all confirmed to be upregulated by use of quantitative real-time RT-PCR (Fig. 6B).

Of the MMP inhibitors, only TIMP1 was upregulated at 2 h (1.7-fold over the level with PG) (Table 1), but it did not stay upregulated at 24 h. This suggests that TDM induces a shift toward an extracellular matrix-degrading phenotype. These results prompted us to pursue the hypothesis that TDM plays a role in the remodeling of tissues during granuloma formation via the induction of MMPs.

TDM induces macrophage-dependent MMP-8 and -9 production and MMP-9 activation. In order to test the hypothesis mentioned above, paraffin-embedded sections of granulomas induced in C57BL/6 mice by the injection of TDM-coated 90-μm-diameter microspheres in Matrigel (BD Biosciences) were examined by IHC for the presence of MMPs. MMP-8 was detected primarily in macrophages in 14-hour-old matrices (Fig. 7), as mice injected with RB6 antibody to deplete neutrophils and a subset of inflammatory macrophages still showed strong staining of macrophages surrounding TDM-coated beads (Fig. 7B). By 36 h, however, only scattered macrophages in the periphery of the matrices (Fig. 7E) stained positively for MMP-8, and by 4 days

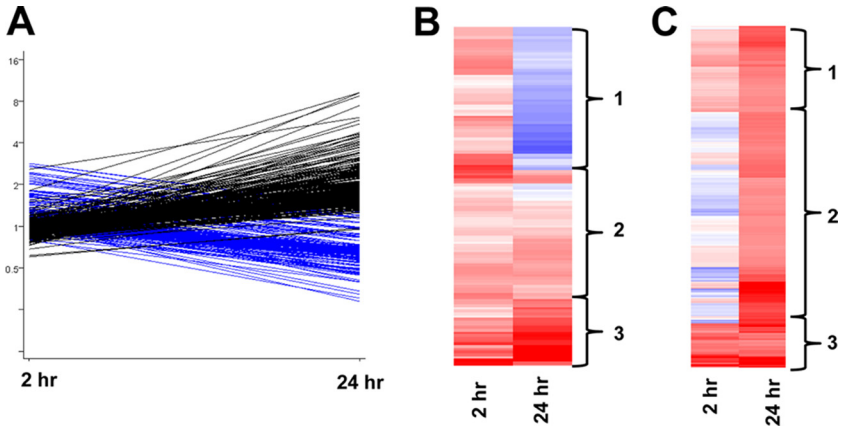

FIG 2 Genes upregulated in response to *M. tuberculosis* H37Rv TDM at 2 or 24 h were compared for movement over time. (A) The line graph shows the distinct movement of most of the genes upregulated at 2 h (blue), going back to control levels of expression, while most of the genes upregulated at 24 h (black) were not upregulated at 2 h. (B) Heat map of genes upregulated at least 1.5-fold at 2 h clustered into 3 groups with regard to expression at 24 h: 1 = downregulated at 24 h, 2 = sustained at 24 h, and 3 = further upregulated at 24 h. (C) Heat map of genes upregulated at least 1.5-fold at 24 h also clustered into 3 groups with regard to expression at 2 h: 1 = further upregulated at 24 h, 2 = upregulated only at 24 h, and 3 = sustained upregulation between 2 and 24 h. Only genes with *P* values of <0.05 are shown.

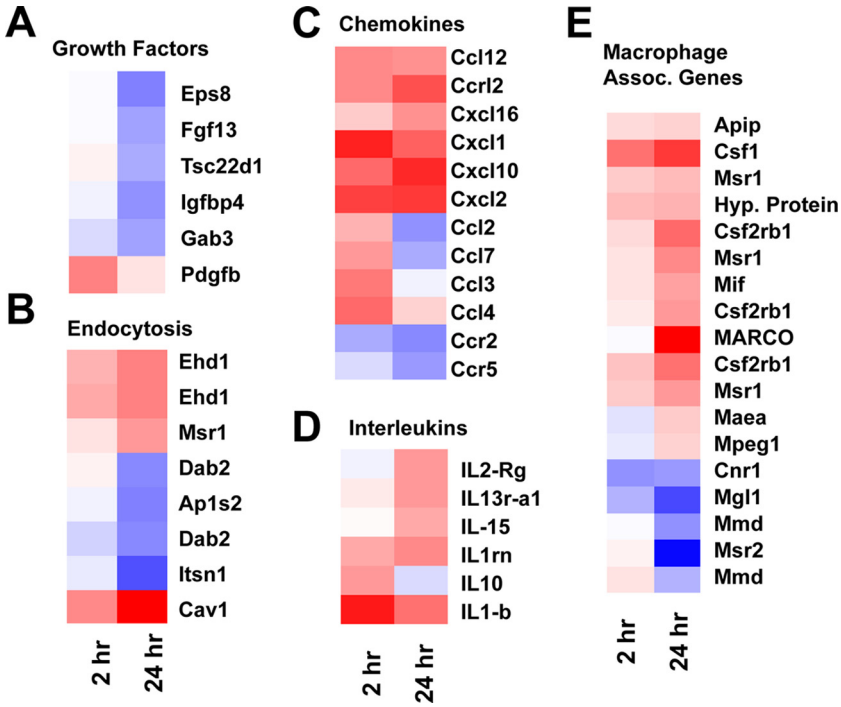

FIG 3 Genes of particular relevance to the immune response and tissue remodeling from the heat maps shown in Fig. 2 are expanded to show individual genes. (A) Several growth factors were specifically downregulated at 24 h in response to TDM-coated beads. (B) Genes involved in endocytosis were variably regulated. (C) Chemokines were also differentially regulated over time, although several, mainly in the CXCL structural group, were upregulated in a sustained fashion. (D) Several interleukins were upregulated between 2 and 24 h, while IL-10 was specifically downregulated over this period and IL-1β responses were slightly reduced at 24 h compared to 2 h. (E) Macrophage-associated genes were also differentially regulated over time. A point of interest is the marked upregulation of MARCO at 24 h.

(Fig. 7F), no staining was observed. MMP-9, on the other hand, was detected for as long as 7 days (Fig. 8A). MMP-13 was not detected at any of the time points examined (data not shown), and MMP-12 and MMP-14 antibodies suitable for IHC could not be obtained at the time of this experiment.

Because MMPs can be present in tissues in an inactive state, the detection of activated MMPs by ISZ is much more informative. Since MMP-9 was identified as present in TDM bead-induced granulomas over an extended period, we decided to focus on MMP-9 for ISZ. ISZ protocols for the detection of activated gelatinases (MMP-2 and -9) are also the best described and are based on the detection of a dye-quenched fluorescent molecule after cleavage from gelatin. For this set of experiments, the TDM granuloma model had to be modified due to the need for cryosections and in order to assess MMP-9 activity induced by recruited leukocytes (as opposed to input BMMΦ). In the modified version, 10-μm-diameter TDM-coated polystyrene microspheres, which still elicit an inflammatory reaction (8), were used because 90-μm-diameter microspheres are not amenable to cryosectioning, no BMMΦ were added, and the mixture was injected into the subcutis of the scruff of C57BL/6 mice because 10-μm-diameter microspheres will not allow a cohesive matrix to be formed in the peritoneal cavity and later retrieved. After 7 or 12 days, the matrices were removed and processed for ISZ. Strong fluorescence was observed at both 7 (Fig. 9A) and 12 (Fig. 9C) days that was mediated primarily by MMP-9, since fluorescence was almost completely eliminated by the presence of an MMP-9 inhibitor (Fig. 9B and D). These results show that TDM-induced MMP-9 gene upregulation correlates with the presence and activation of MMP-9 within TDM-induced granulomas. Furthermore, TIMP1 induction by the TDM-coated beads, as observed in our microarray analysis, was not sufficient to block MMP-9 activity *in situ*.

TABLE 3 BMMΦ genes downregulated at least 2-fold in response to H37Rv TDM-coated beads compared to PG-coated beads at 24 h[a]

Functional category and gene product	Fold change
Immune response	
Ndrg1	2.78
Mrc1	2.44
Msr2	3.7
CCR2	2.44
Thbd	2.22
Tissue remodeling	
Plau	2.08
Rnase4	2.38
Fn1	2.56

[a] Data for replicate genes were averaged.

MMP-9 and MARCO are also highly upregulated in caseous human pulmonary TB granulomas. Our observation that TDM induces the upregulation of MMPs in murine macrophages *in vitro* and *in situ* led us to investigate whether *M. tuberculosis* infection affects the regulation of MMP expression in the human host. For this study, we mined previous data from a genomewide microarray analysis of caseous granulomas, which represent a histologically defined structure of active TB disease (9). Compared to uninvolved lung parenchyma, the transcriptional profiles of caseous human pulmonary TB granulomas revealed top biological

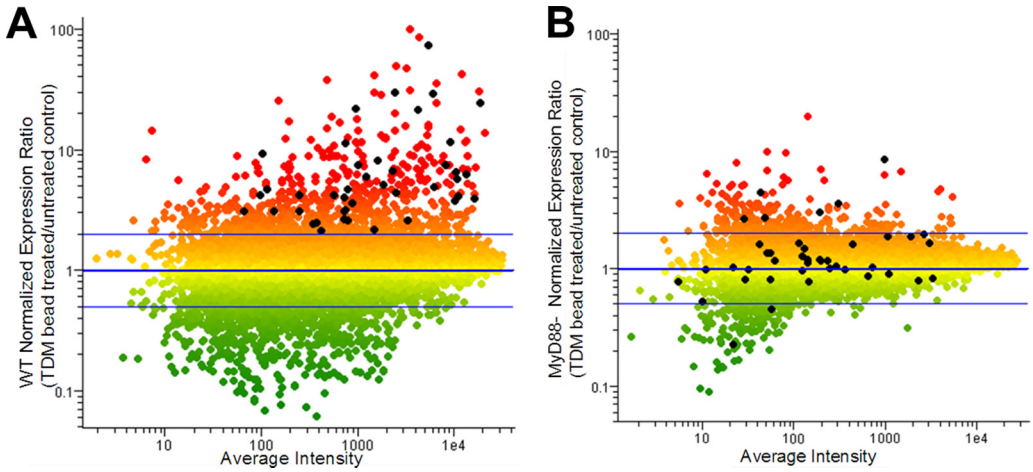

FIG 4 Most of the immune response genes upregulated in response to TDM are MyD88 dependent. BMMΦ from MyD88-deficient and wild-type mice were stimulated with TDM-coated microspheres for 24 h, and gene responses were compared to those of resting BMMΦ from the same genotype. (A) Wild-type BMMΦ showed tremendous up- and downregulation of genes in response to TDM. Black dots indicate genes involved in immune responses. (B) MyD88-deficient mice showed a muted response to TDM-coated beads, and many of the immune response genes were no longer significantly elevated. Threshold bars are set at a 2-fold increase and decrease. Only genes with *P* values of <0.05 are shown.

functions, including cell death, cell-mediated immune response, tissue morphology, and infection mechanisms. MMP-9 was consistently highly expressed in the TB granulomas, while being undetectable in uninvolved regions of the lung. Furthermore, among differentially regulated genes, MARCO, the macrophage scavenger receptor that interacts with TDM (30), was also highly upregulated in the caseous human pulmonary TB granulomas, while being undetectable in uninvolved human lung tissue.

Cryosections were also examined for MMP-9 activation, using DQ-gelatin ISZ. Although there was a high background due to autofluorescence of the elastin in alveolar septa (Fig. 10C), the fluorescence intensity was greater in inflamed lesions overlaid with DQ-gelatin (Fig. 10A) than in those overlaid with gelatin only (Fig. 10B). These data show that gelatinases (MMP-2 or MMP-9) are present and active within human TB lesions, consistent with the microarray data.

In summary, our microarray and ISZ studies of human TB granulomas clearly demonstrate that tissue remodeling is very active in these granulomas at the transcriptional and functional levels, as shown by the upregulation of MMP-9 and cleavage of DQ-gelatin. These data strongly suggest that TDM might contribute to the increased secretion of active MMPs within human TB granulomas, and ultimately to the breakdown of the fibrous TB granuloma capsule, leading to disease transmission.

DISCUSSION

TDM has been shown to have a variety of immunostimulatory properties, such as adjuvanticity (40–43) and enhancement of

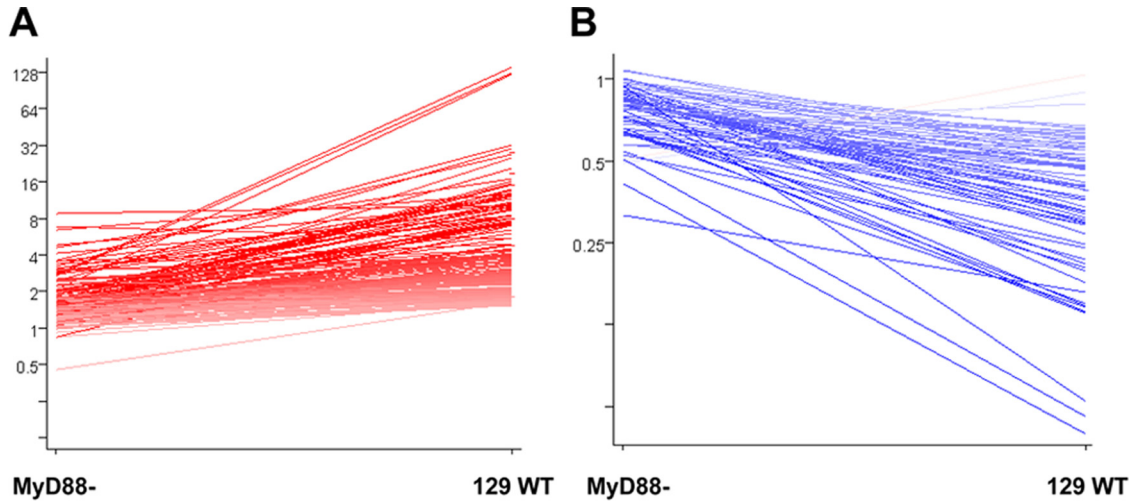

FIG 5 Most of the macrophage genes regulated in response to TDM are MyD88 dependent. BMMΦ genes that were shown to be up- or downregulated in response to H37Rv TDM after normalization against PG were analyzed in the microarray data acquired by the comparison of MyD88-deficient to wild-type BMMΦ. Most genes upregulated (A) or downregulated (B) in response to H37Rv TDM were found to be MyD88 dependent.

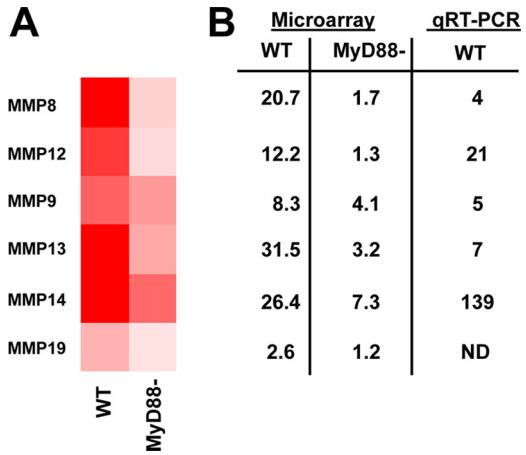

FIG 6 The expression of several MMPs is upregulated at 24 h, in a partially MyD88-dependent manner, in response to stimulation with TDM-coated microspheres. (A) Heat map of gene upregulation in wild-type compared to MyD88-deficient BMMΦ in response to stimulation with TDM for 24 h. (B) Fold upregulation of MMPs in the wild-type versus MyD88-deficient BMMΦ microarray experiment compared to real-time PCR results. ND, not determined.

nonspecific resistance to a number of infectious agents (44–49). While mechanisms for the toxic effects of TDM have been studied in detail, less is known regarding how TDM stimulates macrophages to become activated. Our laboratory, the Hunter laboratory, and others have shown that the mode of presentation of TDM is vital to *in vitro* and *in vivo* responses (6, 8). Micellar and phagocytosable forms of TDM elicit minimal macrophage activation, while oil-water emulsions of TDM and large TDM-coated, nonphagocytosable particles stimulate strong proinflammatory cytokine production from macrophages and robust inflammatory

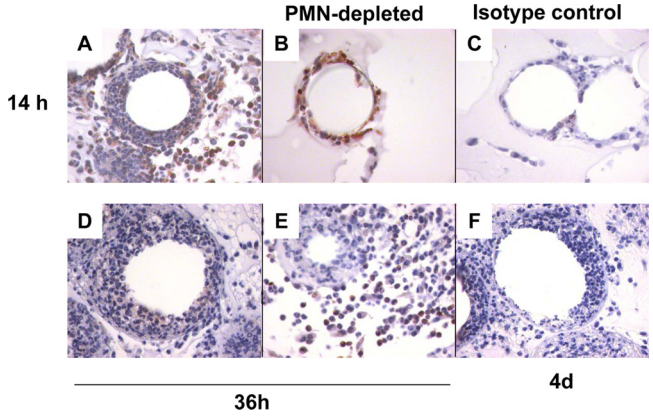

FIG 7 MMP-8 can be detected transiently in TDM-coated bead matrices. TDM-coated 90-μm-diameter microspheres and congenic BMMΦ suspended in Matrigel were injected into the peritoneal cavities of C57BL/6 mice. At various time points, the matrices were removed, fixed, and embedded in paraffin for sectioning and immunohistochemistry. Fourteen-hour-old matrices showed the strongest staining using anti-MMP-8 antibody (A), and this was mostly due to macrophages, as matrices removed from neutrophil-depleted mice still stained strongly (B). (C) An isotype-matched antibody was used as a negative control. (D) By 36 h, few of the cells clustered around the TDM beads stained positively for MMP-8, although scattered cells in the loose periphery of the matrix were positive (E). (F) Very few MMP-8-positive cells remained by 4 days.

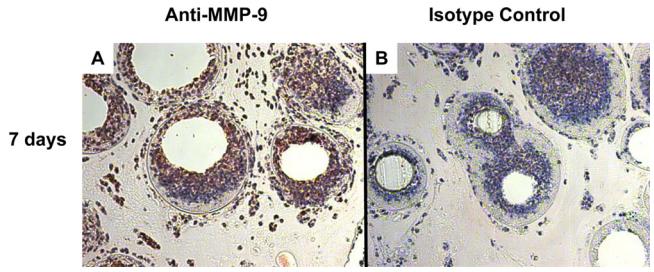

FIG 8 Recruited leukocytes in 7-day-old matrices stain strongly for MMP-9. TDM bead matrices were removed from the peritoneal cavities of mice after 7 days and immunohistochemically stained using anti-MMP-9 antibody. (A) Most of the leukocytes recruited to the TDM-coated beads (open spaces) stained strongly for MMP-9. (B) An isotype-matched control antibody was used as a negative control.

responses *in vivo*. Since we have previously shown that TDM-coated 90-μm-diameter polystyrene microspheres are immunostimulatory for murine BMMΦ in a manner most consistent with *in vivo* administration of TDM in emulsions, we decided to study the regulation of genes during this response in order to better understand the effect of TDM on macrophages.

Our microarray analyses have shown that TDM presented in this manner induces a unique set of genes involved in inflammation, tissue remodeling, and other responses in BMMΦ, in a predominantly MyD88-dependent manner. These results support our previous work showing that TDM at least partially signals through a TLR2 pathway, in association with MARCO and CD14 (30). Comparison of our gene list to genes induced in macrophages from the same mouse strain and at the same time point by lipopolysaccharide (LPS), another ligand that partially signals through the adaptor molecule MyD88, showed only 7 genes in common (50). This discrepancy suggests that receptors and pathways other than the TLR4-MyD88 pathway are utilized by TDM on BMMΦ, although other factors, such as the method of LPS delivery (in solution) and TRIF signaling (the other TLR4 signaling pathway), may also be important. A likely possibility is the FcRγ-Syk-Card9 pathway, mediated by the interaction of TDM

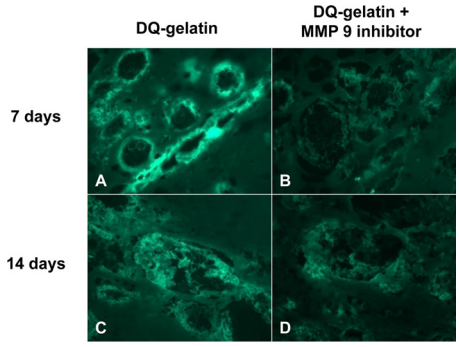

FIG 9 Gelatinase activity in TDM bead granulomas is due primarily to MMP-9 activation. TDM-coated bead-based matrices were removed from the subcutis of C57BL/6 mice after 7 (A and B) and 14 (C and D) days. ISZ was performed on cryosections, using DQ-gelatin as a substrate and a specific MMP-9 inhibitor that distinguishes between MMP-2 and MMP-9 activities. Both time points showed strong activity (A and C) based on release of the fluorescent DQ molecule, which was primarily MMP-9 mediated, as indicated by markedly reduced fluorescence in the presence of an MMP-9 inhibitor (B and D).

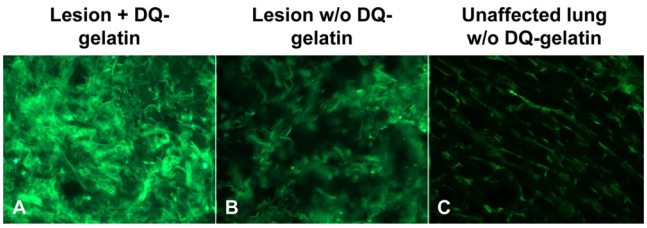

FIG 10 Human tuberculous pulmonary granulomas show gelatinase activity. Cryosections of tuberculous lung samples from human patients were examined by ISZ for gelatinase activity. (A) Gelatinase activity was present within TB granulomas. (B) In the absence of DQ-gelatin, granulomas were autofluorescent due to the presence of elastin; however, these tissues were not fluorescent to the level seen in panel A. (C) Autofluorescence of histologically unremarkable pulmonary architecture.

with the macrophage C-type lectin receptor Mincle (38). Recent *in vivo* infection studies, however, have shown that neither MARCO nor Mincle is required for control of *M. tuberculosis* infection in the mouse model (51, 52), suggesting that there are redundant pathways through which *M. tuberculosis* stimulates the host immune response. Upregulation of several cytokines (TNF-α, IL-1β, and IL-10) and chemokines (CCL3, CCL4, CCL7, CCL12, CXCL1, CXCL2, and CXCL10) important in the response to TB at least partially explains the ability of TDM to induce many of the lesions and symptoms observed during TB (4, 5, 53–58). Several of these immune response genes were also shown to be upregulated by infection with *M. tuberculosis* both *in vitro* and *in vivo* (Table 4) (59–61). These similarities suggest that TDM likely plays a major role in the pathogenesis of TB. It is important, however, that differences between these lists could be due to differences in time points, host species, or the presence of many other immunomodulators on the surface of *M. tuberculosis*.

The mechanism by which late-stage TB granulomas cavitate and rupture is largely unknown. Loss of granuloma regulation by T lymphocytes plays an important role, since depletion of $CD4^+$ T cells during simian immunodeficiency virus infection in macaques results in reactivation of TB (62). Breakdown of the fibrous capsule, however, would require the activation of matrix metalloproteinases, and how this occurs is currently unclear. Microbial products and other TLR agonists that activate macrophages would presumably be able to stimulate the upregulation and activation of MMPs. Furthermore, several MMPs have been shown to be present and/or activated in TB. Other mycobacterial components, such as lipomannan, lipoarabinomannan, and secreted proteins, induce MMP-9 in monocyte cell lines (17, 25, 63). This is the first study, however, to link TDM with MMP induction and activation.

Why microbial products that are persistently present would suddenly induce MMP activation and granuloma cavitation, however, is currently unknown. For example, MMP-9 has already been shown to play an important early role in the development of granulomas during *M. tuberculosis* infection (64). The dependence of TDM on the mode of presentation for its effects, however, makes TDM a unique candidate for this kind of differential immunomodulation. We propose that TDM is relatively immunologically silent during initial infection, since it is presented on the surface of a 1- to 4-μm-long bacillus (65), and our work has shown that TDM presented on microspheres with a diameter of <10 μm is not immunostimulatory (8). As a granuloma becomes more caseous, however, this central debris contains a large amount of undegraded lipids, which could contain TDM. Furthermore, for currently unknown reasons, late-stage granulomas often contain *M. tuberculosis* that resumes active replication, and virulent *M. tuberculosis* will form cords due to the presence of TDM (66). This would present a greater surface area of TDM to macrophages in the granuloma, rapidly triggering the release of MMPs that could then break down the fibrous capsule. Microarray analysis of *in vivo* TDM bead granulomas and caseous human TB granulomas showed that MMP upregulation occurs in both scenarios.

In this study, we have shown that TDM can induce and activate at least MMP-9 *in vivo* in a granuloma model. In order to prove our hypothesis, however, we would need to prove that TDM is present over a large surface area on late-stage granulomas. Polyclonal and monoclonal antibodies produced against TDM, however, are not specific for TDM and recognize other lipids, such as trehalose monomycolate, from the same species, since these antibodies recognize the mycolic acids, which are not unique to TDM (data not shown). Lastly, infection models cannot be used to study the role of TDM in the various stages of the granuloma because mycobacteria deficient in the enzymes required for TDM biosynthesis are not viable, and the mutant bacteria also do not make other trehalose mycolates (67–69). It would be very interesting, however, to follow granuloma development after infection with the cyclopropane-deficient *pcaA* mutant strain of *M. tuberculosis* in an animal model that develops cavitating granulomas, since this mutant produces a less immunostimulatory version of TDM (70) and was shown to be attenuated for up to 130 days in mice, which typically do not form cavitating lesions in response to infection (71). Conversely, the cyclopropane-mycolic acid synthase 2 (*cmaA2*) mutant of *M. tuberculosis*, which lacks *trans*-cyclopropanation of mycolic acids and has been shown to be hypervirulent, may also be interesting to study in a cavitating granuloma model (72). With the development of better staining methods for *M. tuberculosis*, which show that there are more bacteria present in late-stage granulomas than previously detected by traditional acid-fast stains (73), large aggregates of bacteria presenting TDM over a large surface area may be detectable.

TABLE 4 Genes upregulated in response to H37Rv TDM-coated beads at 2 h were also present at 24 h in infection studies[a]

TDM-upregulated gene product	Presence of product (reference)		
	M. tuberculosis infection of C57BL/6 BMMΦ at 24 h (59)	H37Rv infection of C57BL/6 mice at 24 h (60)	Human lung TB infection (61)
ICAM-1			+
IL-1β		+	+
IL-1RA	+		
IER-3		+	
IRG-1		+	
IRF-1			+
Jun-B			+
Nfkbia		+	
SAA3		+	
SOD2	+		
TNF-α		+	
TRAF-1	+		

[a] Genes upregulated at least 1.5-fold in response to TDM-coated beads compared to PG-coated beads at 2 h were compared to gene upregulation in response to infection.

Future work toward understanding the role of TDM in MMP activities needs to include the study of MMP regulators, such as TIMPs. TIMPs form a 1:1 reversible stoichiometric complex with MMPs, and while TIMP1 can inhibit all MMPs, it is considered the primary inhibitor for MMP-9 (74–76). TIMP1 has been shown to be a poor inhibitor of membrane-attached MMP-14 (77), which was especially upregulated in response to TDM (Table 1). Of the MMP inhibitors, however, only TIMP1 was upregulated by TDM, and ISZ results support the observation that this upregulation was not enough to impair MMP-9 activity.

Overall, TDM elicits a robust inflammatory gene profile in macrophages that is particularly consistent with responses to *M. tuberculosis* infection and may be a key driver of the tissue remodeling that occurs during early granuloma formation and late-stage cavitation. These pathological activities suggest that perhaps modification of TDM should be considered during attenuated vaccine design and that prevention of bacterial aggregation may help in the prevention of cavitation and transmission. Further work is needed, however, to definitively show the connection between the form of TDM and granuloma construction and breakdown.

ACKNOWLEDGMENTS

We thank the Core Microarray Facility and the Transgenic Mouse Facility at Cornell University, Patricia Fisher for immunohistochemistry assistance, Eric Denkers for providing us with RB6 antibody, and Cassandra Streeter for assistance in TDM purification. We thank Fong Hsu at Washington University for mass spectrometry confirmation of our purified TDM.

This work was supported in part by U.S. Public Health Service grants HL055936 and AI067027 to D.G.R.

REFERENCES

1. **World Health Organization.** 2011. Global tuberculosis control. World Health Organization, Geneva, Switzerland.
2. **Dannenberg AM, Jr, Sugimoto M.** 1976. Liquefaction of caseous foci in tuberculosis. Am. Rev. Respir. Dis. **113**:257–259.
3. **Witmer G, Fine AE, Gionfriddo J, Pipas M, Shively K, Piccolo K, Burke P.** 2010. Epizootiologic survey of Mycobacterium bovis in wildlife and farm environments in northern Michigan. J. Wildl. Dis. **46**:368–378.
4. **Bekierkunst A.** 1968. Acute granulomatous response produced in mice by trehalose-6,6-dimycolate. J. Bacteriol. **96**:958–961.
5. **Bekierkunst A, Levij IS, Yarkoni E, Vilkas E, Adam A, Lederer E.** 1969. Granuloma formation induced in mice by chemically defined mycobacterial fractions. J. Bacteriol. **100**:95–102.
6. **Retzinger GS, Meredith SC, Takayama K, Hunter RL, Kezdy FJ.** 1981. The role of surface in the biological activities of trehalose 6,6′-dimycolate. Surface properties and development of a model system. J. Biol. Chem. **256**:8208–8216.
7. **Rhoades ER, Geisel RE, Butcher BA, McDonough S, Russell DG.** 2005. Cell wall lipids from Mycobacterium bovis BCG are inflammatory when inoculated within a gel matrix: characterization of a new model of the granulomatous response to mycobacterial components. Tuberculosis (Edinb.) **85**:159–176.
8. **Geisel RE, Sakamoto K, Russell DG, Rhoades ER.** 2005. In vivo activity of released cell wall lipids of Mycobacterium bovis bacillus Calmette-Guerin is due principally to trehalose mycolates. J. Immunol. **174**:5007–5015.
9. **Kim MJ, Wainwright HC, Locketz M, Bekker LG, Walther GB, Dittrich C, Visser A, Wang W, Hsu FF, Wiehart U, Tsenova L, Kaplan G, Russell DG.** 2010. Caseation of human tuberculosis granulomas correlates with elevated host lipid metabolism. EMBO Mol. Med. **2**:258–274.
10. **Parks WC, Wilson CL, Lopez-Boado YS.** 2004. Matrix metalloproteinases as modulators of inflammation and innate immunity. Nat. Rev. **4**:617–629.
11. **Lai WC, Zhou M, Shankavaram U, Peng G, Wahl LM.** 2003. Differential regulation of lipopolysaccharide-induced monocyte matrix metalloproteinase (MMP)-1 and MMP-9 by p38 and extracellular signal-regulated kinase 1/2 mitogen-activated protein kinases. J. Immunol. **170**:6244–6249.
12. **Van Wart HE, Birkedal-Hansen H.** 1990. The cysteine switch: a principle of regulation of metalloproteinase activity with potential applicability to the entire matrix metalloproteinase gene family. Proc. Natl. Acad. Sci. U. S. A. **87**:5578–5582.
13. **Nagase H, Visse R, Murphy G.** 2006. Structure and function of matrix metalloproteinases and TIMPs. Cardiovasc. Res. **69**:562–573.
14. **Visse R, Nagase H.** 2003. Matrix metalloproteinases and tissue inhibitors of metalloproteinases: structure, function, and biochemistry. Circ. Res. **92**:827–839.
15. **Barmina OY, Walling HW, Fiacco GJ, Freije JM, Lopez-Otin C, Jeffrey JJ, Partridge NC.** 1999. Collagenase-3 binds to a specific receptor and requires the low density lipoprotein receptor-related protein for internalization. J. Biol. Chem. **274**:30087–30093.
16. **Fu X, Kassim SY, Parks WC, Heinecke JW.** 2003. Hypochlorous acid generated by myeloperoxidase modifies adjacent tryptophan and glycine residues in the catalytic domain of matrix metalloproteinase-7 (matrilysin): an oxidative mechanism for restraining proteolytic activity during inflammation. J. Biol. Chem. **278**:28403–28409.
17. **Rivera-Marrero CA, Schuyler W, Roser S, Roman J.** 2000. Induction of MMP-9 mediated gelatinolytic activity in human monocytic cells by cell wall components of Mycobacterium tuberculosis. Microb. Pathog. **29**:231–244.
18. **Quiding-Jarbrink M, Smith DA, Bancroft GJ.** 2001. Production of matrix metalloproteinases in response to mycobacterial infection. Infect. Immun. **69**:5661–5670.
19. **Chang JC, Wysocki A, Tchou-Wong KM, Moskowitz N, Zhang Y, Rom WN.** 1996. Effect of Mycobacterium tuberculosis and its components on macrophages and the release of matrix metalloproteinases. Thorax **51**:306–311.
20. **Hoheisel G, Sack U, Hui DS, Huse K, Chan KS, Chan KK, Hartwig K, Schuster E, Scholz GH, Schauer J.** 2001. Occurrence of matrix metalloproteinases and tissue inhibitors of metalloproteinases in tuberculous pleuritis. Tuberculosis (Edinb.) **81**:203–209.
21. **Park KJ, Hwang SC, Sheen SS, Oh YJ, Han JH, Lee KB.** 2005. Expression of matrix metalloproteinase-9 in pleural effusions of tuberculosis and lung cancer. Respiration **72**:166–175.
22. **Elkington PT, Nuttall RK, Boyle JJ, O'Kane CM, Horncastle DE, Edwards DR, Friedland JS.** 2005. Mycobacterium tuberculosis, but not vaccine BCG, specifically upregulates matrix metalloproteinase-1. Am. J. Respir. Crit. Care Med. **172**:1596–1604.
23. **Elkington P, Shiomi T, Breen R, Nuttall RK, Ugarte-Gil CA, Walker NF, Saraiva L, Pedersen B, Mauri F, Lipman M, Edwards DR, Robertson BD, D'Armiento J, Friedland JS.** 2011. MMP-1 drives immunopathology in human tuberculosis and transgenic mice. J. Clin. Invest. **121**:1827–1833.
24. **Hrabec E, Strek M, Zieba M, Kwiatkowska S, Hrabec Z.** 2002. Circulation level of matrix metalloproteinase-9 is correlated with disease severity in tuberculosis patients. Int. J. Tuberc. Lung Dis. **6**:713–719.
25. **Volkman HE, Pozos TC, Zheng J, Davis JM, Rawls JF, Ramakrishnan L.** 2010. Tuberculous granuloma induction via interaction of a bacterial secreted protein with host epithelium. Science **327**:466–469.
26. **Takayama K, Schnoes HK, Armstrong EL, Boyle RW.** 1975. Site of inhibitory action of isoniazid in the synthesis of mycolic acids in Mycobacterium tuberculosis. J. Lipid Res. **16**:308–317.
27. **Rhoades E, Hsu F, Torrelles JB, Turk J, Chatterjee D, Russell DG.** 2003. Identification and macrophage-activating activity of glycolipids released from intracellular Mycobacterium bovis BCG. Mol. Microbiol. **48**:875–888.
28. **Wipke BT, Allen PM.** 2001. Essential role of neutrophils in the initiation and progression of a murine model of rheumatoid arthritis. J. Immunol. **167**:1601–1608.
29. **Shi C, Hohl TM, Leiner I, Equinda MJ, Fan X, Pamer EG.** 2011. Ly6G+ neutrophils are dispensable for defense against systemic Listeria monocytogenes infection. J. Immunol. **187**:5293–5298.
30. **Bowdish DM, Sakamoto K, Kim MJ, Kroos M, Mukhopadhyay S, Leifer CA, Tryggvason K, Gordon S, Russell DG.** 2009. MARCO, TLR2, and CD14 are required for macrophage cytokine responses to mycobacterial trehalose dimycolate and Mycobacterium tuberculosis. PLoS Pathog. **5**:e1000474. doi:10.1371/journal.ppat.1000474.
31. **Nan B, Lin P, Lumsden AB, Yao Q, Chen C.** 2005. Effects of TNF-alpha

and curcumin on the expression of thrombomodulin and endothelial protein C receptor in human endothelial cells. Thromb. Res. **115**:417–426.
32. **Flynn JL, Goldstein MM, Chan J, Triebold KJ, Pfeffer K, Lowenstein CJ, Schreiber R, Mak TW, Bloom BR.** 1995. Tumor necrosis factor-alpha is required in the protective immune response against Mycobacterium tuberculosis in mice. Immunity **2**:561–572.
33. **Chen YC, Chin CH, Liu SF, Wu CC, Tsen CC, Wang YH, Chao TY, Lie CH, Chen CJ, Wang CC, Lin MC.** 2011. Prognostic values of serum IP-10 and IL-17 in patients with pulmonary tuberculosis. Dis. Markers **31**:101–110.
34. **Sarkar S, Song Y, Sarkar S, Kipen HM, Laumbach RJ, Zhang J, Strickland PA, Gardner CR, Schwander S.** 2012. Suppression of the NF-kappaB pathway by diesel exhaust particles impairs human antimycobacterial immunity. J. Immunol. **188**:2778–2793.
35. **Liu E, Law HK, Lau YL.** 2003. BCG promotes cord blood monocyte-derived dendritic cell maturation with nuclear Rel-B up-regulation and cytosolic I kappa B alpha and beta degradation. Pediatr. Res. **54**:105–112.
36. **Windish HP, Lin PL, Mattila JT, Green AM, Onuoha EO, Kane LP, Flynn JL.** 2009. Aberrant TGF-beta signaling reduces T regulatory cells in ICAM-1-deficient mice, increasing the inflammatory response to Mycobacterium tuberculosis. J. Leukoc. Biol. **86**:713–725.
37. **Dutta NK, Mehra S, Martinez AN, Alvarez X, Renner NA, Morici LA, Pahar B, Maclean AG, Lackner AA, Kaushal D.** 2012. The stress-response factor SigH modulates the interaction between Mycobacterium tuberculosis and host phagocytes. PLoS One **7**:e28958. doi:10.1371/journal.pone.0028958.
38. **Schoenen H, Bodendorfer B, Hitchens K, Manzanero S, Werninghaus K, Nimmerjahn F, Agger EM, Stenger S, Andersen P, Ruland J, Brown GD, Wells C, Lang R.** 2010. Cutting edge: Mincle is essential for recognition and adjuvanticity of the mycobacterial cord factor and its synthetic analog trehalose-dibehenate. J. Immunol. **184**:2756–2760.
39. **Ishikawa E, Ishikawa T, Morita YS, Toyonaga K, Yamada H, Takeuchi O, Kinoshita T, Akira S, Yoshikai Y, Yamasaki S.** 2009. Direct recognition of the mycobacterial glycolipid, trehalose dimycolate, by C-type lectin Mincle. J. Exp. Med. **206**:2879–2888.
40. **Bekierkunst A, Yarkoni E, Flechner I, Morecki S, Vilkas E, Lederer E.** 1971. Immune response to sheep red blood cells in mice pretreated with mycobacterial fractions. Infect. Immun. **4**:256–263.
41. **Granger DL, Yamamoto KI, Ribi E.** 1976. Delayed hypersensitivity and granulomatous response after immunization with protein antigens associated with a mycobacterial glycolipid and oil droplets. J. Immunol. **116**:482–488.
42. **Saito R, Nagao S, Takamoto M, Sugiyama K, Tanaka A.** 1977. Adjuvanticity (immunity-inducing property) of cord factor in mice and rats. Infect. Immun. **16**:725–729.
43. **Saito R, Tanaka A, Sugiyama K, Azuma I, Yamamura Y.** 1976. Adjuvant effect of cord factor, a mycobacterial lipid. Infect. Immun. **13**:776–781.
44. **Yarkoni E, Bekierkunst A.** 1976. Nonspecific resistance against infection with Salmonella typhi and Salmonella typhimurium induced in mice by cord factor (trehalose-6,6′-dimycolate) and its analogues. Infect. Immun. **14**:1125–1129.
45. **Madonna GS, Ledney GD, Elliott TB, Brook I, Ulrich JT, Myers KR, Patchen ML, Walker RI.** 1989. Trehalose dimycolate enhances resistance to infection in neutropenic animals. Infect. Immun. **57**:2495–2501.
46. **Guillemard E, Geniteau-Legendre M, Kergot R, Lemaire G, Petit JF, Labarre C, Quero AM.** 1995. Role of trehalose dimycolate-induced interferon-alpha/beta in the restriction of encephalomyocarditis virus growth in vivo and in peritoneal macrophage cultures. Antiviral Res. **28**:175–189.
47. **Kierszenbaum F, Zenian A, Wirth JJ.** 1984. Macrophage activation by cord factor (trehalose 6,6′-dimycolate): enhanced association with and intracellular killing of Trypanosoma cruzi. Infect. Immun. **43**:531–535.
48. **Clark IA.** 1979. Protection of mice against Babesia microti with cord factor, COAM, zymosan, glucan, Salmonella and Listeria. Parasite Immunol. **1**:179–196.
49. **Masihi KN, Brehmer W, Lange W, Werner H, Ribi E.** 1985. Trehalose dimycolate from various mycobacterial species induces differing anti-infectious activities in combination with muramyl dipeptide. Infect. Immun. **50**:938–940.
50. **Nilsson R, Bajic VB, Suzuki H, di Bernardo D, Bjorkegren J, Katayama S, Reid JF, Sweet MJ, Gariboldi M, Carninci P, Hayashizaki Y, Hume DA, Tegner J, Ravasi T.** 2006. Transcriptional network dynamics in macrophage activation. Genomics **88**:133–142.
51. **Court N, Vasseur V, Vacher R, Fremond C, Shebzukhov Y, Yeremeev VV, Maillet I, Nedospasov SA, Gordon S, Fallon PG, Suzuki H, Ryffel B, Quesniaux VF.** 2010. Partial redundancy of the pattern recognition receptors, scavenger receptors, and C-type lectins for the long-term control of Mycobacterium tuberculosis infection. J. Immunol. **184**:7057–7070.
52. **Heitmann L, Schoenen H, Ehlers S, Lang R, Holscher C.** Mincle is not essential for controlling Mycobacterium tuberculosis infection. Immunobiology, in press.
53. **Chiu BC, Freeman CM, Stolberg VR, Komuniecki E, Lincoln PM, Kunkel SL, Chensue SW.** 2003. Cytokine-chemokine networks in experimental mycobacterial and schistosomal pulmonary granuloma formation. Am. J. Respir. Cell Mol. Biol. **29**:106–116.
54. **Behling CA, Perez RL, Kidd MR, Staton GW, Jr, Hunter RL.** 1993. Induction of pulmonary granulomas, macrophage procoagulant activity, and tumor necrosis factor-alpha by trehalose glycolipids. Ann. Clin. Lab. Sci. **23**:256–266.
55. **Perez RL, Roman J, Roser S, Little C, Olsen M, Indrigo J, Hunter RL, Actor JK.** 2000. Cytokine message and protein expression during lung granuloma formation and resolution induced by the mycobacterial cord factor trehalose-6,6′-dimycolate. J. Interferon Cytokine Res. **20**:795–804.
56. **Actor JK, Indrigo J, Beachdel CM, Olsen M, Wells A, Hunter RL, Jr, Dasgupta A.** 2002. Mycobacterial glycolipid cord factor trehalose 6,6′-dimycolate causes a decrease in serum cortisol during the granulomatous response. Neuroimmunomodulation **10**:270–282.
57. **Hamasaki N, Isowa K, Kamada K, Terano Y, Matsumoto T, Arakawa T, Kobayashi K, Yano I.** 2000. In vivo administration of mycobacterial cord factor (trehalose 6,6′-dimycolate) can induce lung and liver granulomas and thymic atrophy in rabbits. Infect. Immun. **68**:3704–3709.
58. **Silva CL, Faccioli LH.** 1988. Tumor necrosis factor (cachectin) mediates induction of cachexia by cord factor from mycobacteria. Infect. Immun. **56**:3067–3071.
59. **Shi S, Nathan C, Schnappinger D, Drenkow J, Fuortes M, Block E, Ding A, Gingeras TR, Schoolnik G, Akira S, Takeda K, Ehrt S.** 2003. MyD88 primes macrophages for full-scale activation by interferon-gamma yet mediates few responses to Mycobacterium tuberculosis. J. Exp. Med. **198**:987–997.
60. **Keller C, Lauber J, Blumenthal A, Buer J, Ehlers S.** 2004. Resistance and susceptibility to tuberculosis analysed at the transcriptome level: lessons from mouse macrophages. Tuberculosis (Edinb.) **84**:144–158.
61. **Grassi M, Bocchino M, Marruchella A, Volpe E, Saltini C, Colizzi V, Mariani F.** 2006. Transcriptional profile of the immune response in the lungs of patients with active tuberculosis. Clin. Immunol. **121**:100–107.
62. **Shen Y, Shen L, Sehgal P, Huang D, Qiu L, Du G, Letvin NL, Chen ZW.** 2004. Clinical latency and reactivation of AIDS-related mycobacterial infections. J. Virol. **78**:14023–14032.
63. **Elass E, Aubry L, Masson M, Denys A, Guerardel Y, Maes E, Legrand D, Mazurier J, Kremer L.** 2005. Mycobacterial lipomannan induces matrix metalloproteinase-9 expression in human macrophagic cells through a Toll-like receptor 1 (TLR1)/TLR2- and CD14-dependent mechanism. Infect. Immun. **73**:7064–7068.
64. **Taylor JL, Hattle JM, Dreitz SA, Troudt JM, Izzo LS, Basaraba RJ, Orme IM, Matrisian LM, Izzo AA.** 2006. Role for matrix metalloproteinase 9 in granuloma formation during pulmonary Mycobacterium tuberculosis infection. Infect. Immun. **74**:6135–6144.
65. **Kaneda K, Imaizumi S, Mizuno S, Baba T, Tsukamura M, Yano I.** 1988. Structure and molecular species composition of three homologous series of alpha-mycolic acids from Mycobacterium spp. J. Gen. Microbiol. **134**:2213–2229.
66. **Hunter RL, Olsen M, Jagannath C, Actor JK.** 2006. Trehalose 6,6′-dimycolate and lipid in the pathogenesis of caseating granulomas of tuberculosis in mice. Am. J. Pathol. **168**:1249–1261.
67. **Harth G, Zamecnik PC, Tabatadze D, Pierson K, Horwitz MA.** 2007. Hairpin extensions enhance the efficacy of mycolyl transferase-specific antisense oligonucleotides targeting Mycobacterium tuberculosis. Proc. Natl. Acad. Sci. U. S. A. **104**:7199–7204.
68. **Harth G, Zamecnik PC, Tang JY, Tabatadze D, Horwitz MA.** 2000. Treatment of Mycobacterium tuberculosis with antisense oligonucleotides to glutamine synthetase mRNA inhibits glutamine synthetase activity, formation of the poly-L-glutamate/glutamine cell wall structure, and bacterial replication. Proc. Natl. Acad. Sci. U. S. A. **97**:418–423.
69. **Belisle JT, Vissa VD, Sievert T, Takayama K, Brennan PJ, Besra GS.**

1997. Role of the major antigen of Mycobacterium tuberculosis in cell wall biogenesis. Science **276**:1420–1422.
70. **Rao V, Fujiwara N, Porcelli SA, Glickman MS.** 2005. Mycobacterium tuberculosis controls host innate immune activation through cyclopropane modification of a glycolipid effector molecule. J. Exp. Med. **201**:535–543.
71. **Barkan D, Hedhli D, Yan HG, Huygen K, Glickman MS.** 2012. Mycobacterium tuberculosis lacking all mycolic acid cyclopropanation is viable but highly attenuated and hyperinflammatory in mice. Infect. Immun. **80**:1958–1968.
72. **Rao V, Gao F, Chen B, Jacobs WR, Jr, Glickman MS.** 2006. Trans-cyclopropanation of mycolic acids on trehalose dimycolate suppresses Mycobacterium tuberculosis-induced inflammation and virulence. J. Clin. Invest. **116**:1660–1667.
73. **Ryan GJ, Hoff DR, Driver ER, Voskuil MI, Gonzalez-Juarrero M, Basaraba RJ, Crick DC, Spencer JS, Lenaerts AJ.** 2010. Multiple M. tuberculosis phenotypes in mouse and guinea pig lung tissue revealed by a dual-staining approach. PLoS One **5**:e11108. doi:10.1371/journal.pone.0011108.
74. **Woessner JF, Jr.** 1991. Matrix metalloproteinases and their inhibitors in connective tissue remodeling. FASEB J. **5**:2145–2154.
75. **Henriet P, Blavier L, Declerck YA.** 1999. Tissue inhibitors of metalloproteinases (TIMP) in invasion and proliferation. APMIS **107**:111–119.
76. **Nagase H.** 1997. Activation mechanisms of matrix metalloproteinases. Biol. Chem. **378**:151–160.
77. **d'Ortho MP, Stanton H, Butler M, Atkinson SJ, Murphy G, Hembry RM.** 1998. MT1-MMP on the cell surface causes focal degradation of gelatin films. FEBS Lett. **421**:159–164.